Tetrahedron Letters 51 (2010) 2130–2135

Contents lists available at ScienceDirect

Tetrahedron Letters

journal homepage: www.elsevier.com/locate/tetlet

The efficiency of proton transfer in Kirby's enzyme model, a computational approach

Rafik Karaman *

Faculty of Pharmacy, Al-Quds University, PO Box 20002, Jerusalem, Palestine

ARTICLE INFO

Article history:
Received 15 January 2010
Revised 1 February 2010
Accepted 12 February 2010
Available online 16 February 2010

ABSTRACT

DFT and ab initio calculation results for proton transfer reactions in Kirby's acetals reveal that the mechanism proceeds via efficient intramolecular general acid catalysis (IGAC) and not through a 'classical' general acid catalysis mechanism (GAC). Further, they show that the driving force for the proton transfer efficiency is the proximity of the two reactive centers (r) and the attack angle (α), and the rate of the reaction is linearly correlated with r^2 and sin $(180^\circ - \alpha)$. Acetals with short r values and with α values close to 180° (forming a linear H-bond) are more reactive due to the development of strong hydrogen bonds in their global minimum, transition state, and product structures.

For many years chemists and biochemists have utilized intramolecularity to understand how enzymes accomplish their significant rate enhancements. Intramolecular processes are generally faster and more efficient than their intermolecular counterparts due to the proximity orientation of the two reacting centers which mimics that of functional groups when brought together in the enzyme active site.[1]

Intramolecularity is usually measured by the effective molarity parameter (EM). EM is defined as the rate ratio (k_{intra}/k_{inter}) for corresponding intramolecular and intermolecular processes driven by identical mechanisms. Ring size, solvent, and reaction type are the main factors affecting the effective molarity. Ring-closing reactions via intramolecular nucleophilic addition are much more efficient than intramolecular proton transfer reactions. EM values in the order of 10^9–10^{13} M have been measured for intramolecular processes occurring through nucleophilic addition. Whereas for proton transfer processes values of less than 10 M were obtained.[2]

Recently, we have studied the origin of the driving forces for the significant accelerations in the rates of some important intramolecular processes.[3] Exploiting ab initio and DFT molecular orbital methods, we explored the mechanistic behavior of the acid-catalyzed lactonization of hydroxy-acids as studied by Menger[4] and Cohen,[5] the cyclization reactions of dicarboxylic semi-esters as investigated by Bruice,[6] intramolecular proton-transfers in rigid systems as researched by Menger[4], and S_N2-based ring-closing reactions as studied by Mandolini.[7] Furthermore, using the DFT method, we have established a rationale for calculating the EM values of a variety of intramolecular processes.[8] The main conclusion to emerge from these works is that strained and/or strain-less proximity orientation effects (proximity of an electrophile to a nucleophile) play a crucial role in enhancing or inhibiting the reaction rate.[3,8]

In continuation of our investigations on the driving force responsible for the remarkable accelerations in enzyme models based on intramolecularity, we sought to investigate, using molecular orbital methods, the mode and scope of the efficiency of proton transfer in Kirby's enzyme model (Scheme 1).[9]

In this Letter, we describe our DFT and ab initio quantum molecular orbital investigations of ground state and transition state structures, vibrational frequencies, and reaction trajectories for efficient intramolecular general acid catalysis (IGAC) in five of Kirby's enzyme model systems **1**–**5** (Scheme 1) which show EM values as high as 10^5–10^{10} M.[9] In order to calculate the EM values for **1**–**5**, the intermolecular process for **6** (Scheme 2) was also computed.

The goal of this investigation was to (a) unravel the nature of the driving force(s) for the unprecedented efficiency of the IGAC in **1** (Scheme 1) and (b) locate intramolecular hydrogen bonds in the entities along the reaction pathway (reactants, transition state, and products) and to evaluate their role in the efficiency of the intramolecular process.

Computational efforts were directed toward the elucidation of the transition and ground state structures for the proton transfer processes in **1**–**5** due to the importance of intramolecular hydrogen bonding on the stability of the ground states, the derived transition states, and consequently, the corresponding products.[9]

Using the quantum chemical package GAUSSIAN-98[10], we have calculated the ab initio HF/6-31G and the DFT B3LYP/6-31G (d,p) kinetic and thermodynamic parameters for the IGAC in processes **1**–**5** (Scheme 1) and for the intermolecular processes **6** and **7** (Scheme 2). The intermolecular process **6** was chosen as an intermolecular proton transfer process for calculating the effective

* Tel.: +972 2 523929549; fax: +972 22790413.
E-mail address: dr_karaman@yahoo.com

0040-4039/$ - see front matter © 2010 Elsevier Ltd. All rights reserved.
doi:10.1016/j.tetlet.2010.02.062

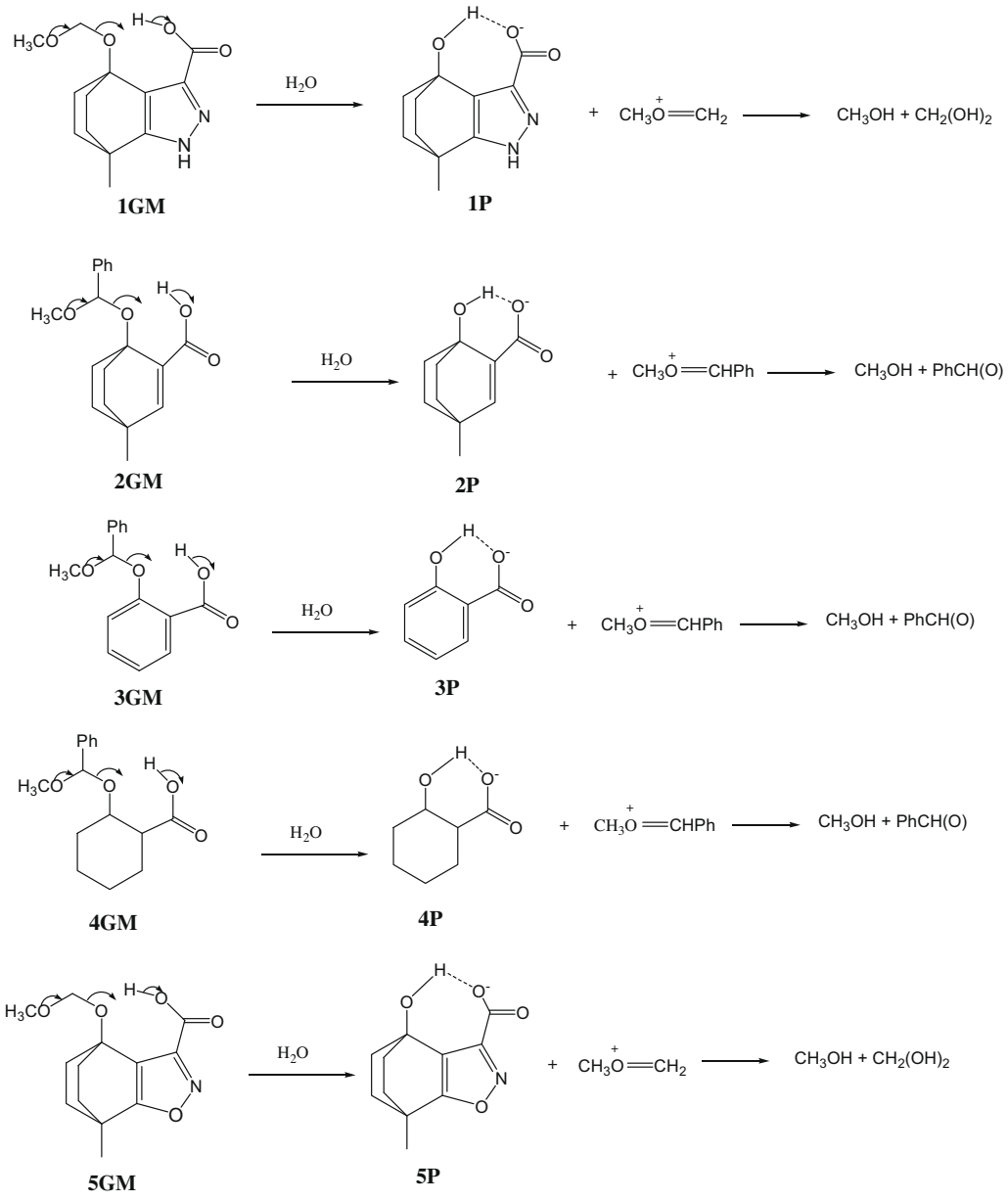

Scheme 1. Proton transfer reactions in **1**–**5**, where GM and P are the reactant and the product, respectively.

molarity values of the corresponding intramolecular processes **1–5**, and process **7** was employed to represent proton transfer driven by 'classical' general acid catalysis (GAC) for comparison with that driven by IGAC (see for example process **1**).

Using the HF and DFT calculated enthalpic and entropic energies for the global minimum structures (GM) of **1**–**6** and the derived transition states (TS) (Table S1, Supplementary data), we have calculated the enthalpic activation energies ($\Delta\Delta H^{\ddagger}$), the entropic activation energies ($T\Delta S^{\ddagger}$), and the free activation energies in the gas phase ($\Delta\Delta G^{\ddagger}$) and in water for the corresponding proton transfer reactions. The calculated kinetic parameters are summarized in Table 1. Table 2 lists the values of the O1–H2 distances and the attack angles O1H2O3 (Fig. 1) for the reactants and the corresponding transition states for processes **1**–**5**. Figures 2 and S1 (Supplementary data) illustrate the DFT calculated global minimum (GM), transition state (TS), and product (P) structures for the proton transfer processes in **1–6**.

Careful examination of the optimized global minimum structures for processes **1–3** and **5** (**1**GM, **2**GM, **3**GM, and **5**GM) revealed the existence of intramolecular hydrogen bonding between the carboxyl hydroxy group O3–H2 and the ether oxygen O1 (Figs. 2 and S1). On the other hand, no intramolecular hydrogen bond was found in the global minimum structure of **4** (**4** GM) (Fig. 2). This is because the carboxyl group in **4** GM prefers to engage in hydrogen bonding with a molecule of water rather than intramolecularly, since the latter will be energetically expensive due to the high energy barrier for rotation of the carboxyl group around the cyclohexyl moiety.[11] It should be emphasized that Fife and coworkers reported that the benzaldehyde acetal **4** shows no IGAC by the neighboring carboxyl group.[12] Further, inspection of Table 2 indicates that the distance between the two reactive centers (O1–H2) varies according to the conformation in which the global minimum structure resides (GM). Short O1–H2 distance values were achieved when the values of the attack angle (α) in the GM conformations were high and close to 180°, whereas small values of α resulted in longer O1–H2 distances.

The optimized structures for processes **1**–**5** (**1**TS-**5**TS and **1**P-**5**P) shown in Figures 2 and S1 indicate the development of intramolec-

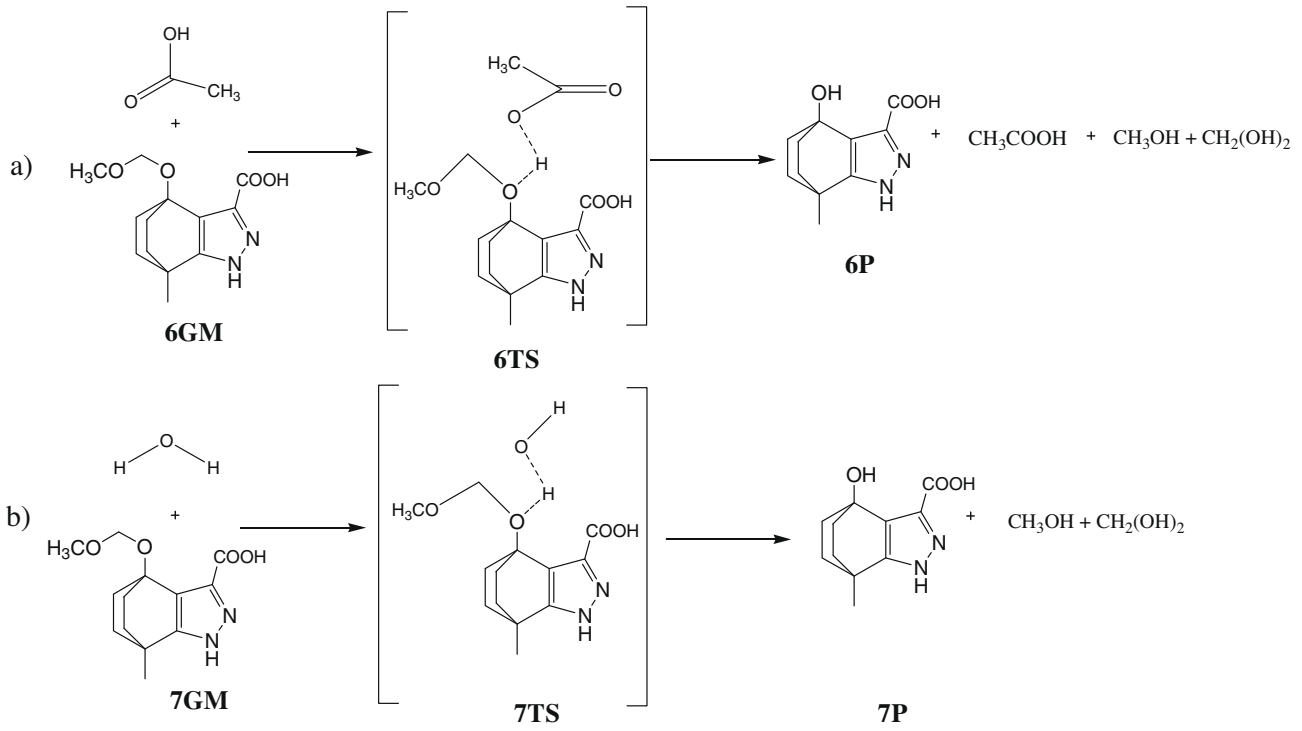

Scheme 2. (a) A representative intermolecular proton transfer reaction of an acetal (Kirby's system) with acetic acid in water; (b) a representative general proton transfer reaction of an acetal (Kirby's system) in water. GM, TS and P are reactant, transition state and product, respectively.

Table 1
HF and DFT (B3LYP) calculated kinetic and thermodynamic properties for the proton transfer in systems **1–7**

System	Medium	HF	HF	HF	B3LYP	B3LYP	B3LYP	B3LYP calculated log EM
		$\Delta H^{\ddagger}$	$T\Delta S^{\ddagger}$	$\Delta G^{\ddagger}$	$\Delta H^{\ddagger}$	$T\Delta S^{\ddagger}$	$\Delta G^{\ddagger}$	
1	Gas phase	26.25	−0.47	26.72	27.78	−2.68	30.46	—
	Water	—	—	—	21.47	−2.68	24.15	10.58
2	Gas phase	30.64	−1.9	32.54	31.38	−3.71	35.09	—
	Water	—	—	—	26.64	−3.71	30.35	6.04
3	Gas phase	33.08	−3.79	36.87	29.04	−5.12	34.16	—
	Water	—	—	—	26.22	−5.12	31.34	5.30
4	Gas phase	38.89	−3.03	41.92	41.09	1.04	40.05	—
	Water	—	—	—	40.15	1.04	39.11	−0.41
5	Gas phase	31.31	−1.77	33.08	29.3	0.03	29.27	—
	Water	—	—	—	21.22	0.03	21.19	12.72
6	Gas phase	44.83	−1.64	46.47	44.60	−2.82	46.82	—
	Water	—	—	—	35.73	−2.82	38.55	0
7	Gas phase	55.96	−3.61	59.57	52.59	−3.93	56.52	—
	Water	—	—	—	49.21	−3.93	53.14	−10.72

HF and B3LYP refer to values calculated by HF/6-31G and B3LYP/6-31G (d, p) methods, respectively. $\Delta H^{\ddagger}$ is the activation enthalpic energy (kcal/mol). $T\Delta S^{\ddagger}$ is the activation entropic energy in kcal/mol.
$\Delta G^{\ddagger}$ is the activation free energy (kcal/mol). EM $= e^{-(\Delta G^{\ddagger}_{inter} - \Delta G^{\ddagger}_{intra})/RT}$.

Table 2
HF and DFT (B3L) calculated properties for the proton transfer in **1–5**

System	HF/GM	HF/GM	HF/TS	B3L/GM	B3L/GM	B3L/TS
	O–H (Å)	O–H–O (°)	O–H–O (°)	O–H (Å)	O–H–O (°)	O–H–O (°)
1	1.67	169	170	1.70	170	170
2	1.71	143	144	1.69	149	144
3	1.77	139	153	1.74	147	153
4	3.62	45	131	3.66	48	131
5	1.72	170	162	1.72	171	162

HF and B3L refer to values calculated using HF/6-31G and B3LYP/6-31G (d, p) methods, respectively. GM and TS refer to global minimum and transition state structures, respectively.

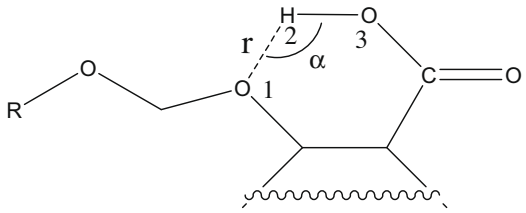

Figure 1. The angle of attack O1H2O3 (α), usually described in terms of the linearity of the H-bond with the two oxygens (O1 and O3), and the distance between the two reacting centers H2–O1 (r) in systems **1**–**5**. R is an alkyl or aryl group.

ular hydrogen bonding in the products and also in the transition states leading to them. It should be emphasized that the minimized transition state and product structures for process **4** (**4**TS and **4**P) involve intramolecular hydrogen bonding. This is contrary to that observed in the corresponding global minimum structure (**4** GM).

Inspection of Tables 1 and 2 reveals that the free activation energy ($\Delta G^{\ddagger}$) in the gas phase and in water needed to execute proton transfer in systems **1–5** is largely affected by both the distance between the two reactive centers r (O1–H2), and the attack angle α (O1H2O3). Systems having low r and high α values in their global minimum structures, such as **1** and **5**, exhibit much higher rates (lower $\Delta G^{\ddagger}$) than those with high r and low α values, such as **4**. Linear correlation of the calculated DFT activation energies ($\Delta G^{\ddagger}$) with sin $(180 - \alpha)$ values gave strong correlations with relatively high correlation coefficients, $R = 0.96$ when the calculations were carried in the gas phase, and 0.97 when they were derived in water (Fig. 3a). However, correlation of the corresponding calculated HF values gave a poor correlation coefficient ($R = 0.77$). On the other hand, the calculated DFT r values ($1/r^2$) were found to correlate much better with the calculated DFT $\Delta H^{\ddagger}$ values than with the corresponding calculated DFT $\Delta G^{\ddagger}$ values (R = 0.96 vs 0.82, Fig. 3b). When the calculated DFT enthalpy energies ($\Delta H^{\ddagger}$) and activation energies ($\Delta G^{\ddagger}$) were examined for correlation with both r and α values, improved correlation coefficients were achieved with the calculated $\Delta H^{\ddagger}$ values ($R = 0.98$ vs 0.88, Fig. 3c).

In a similar manner, correlations of the DFT calculated $\Delta H^{\ddagger}$ and $\Delta G^{\ddagger}$ values with the angle O1H2O3 (β) developed at the transition state furnished strong correlations with a high correlation coefficient ($R = 0.99$ for the calculated values in the gas phase and $R = 0.98$ for those calculated in water as the solvent, Fig. 3d).

The combined results suggest that the structural requirements for a system to achieve a high intramolecular proton transfer reaction rate are (1) a short distance between the two reactive centers (r) in the ground state (GM) which subsequently results in strong intramolecular hydrogen bonding and (2) the attack angle α in the ground state and consequently the angle β in the transition state should be close to 180° in order to maximize the orbital overlap of the two reactive centers when they are engaged along the reaction pathway. Among the five systems that were investigated theoretically, systems **1** and **5** were the most reactive due to the fact that they both fulfill, to a high extent, the two requirements ($\alpha = 170°$ and $r = 1.7$ Å). System **4** has the lowest rate as a result of having an angle of attack and distance between the two reactive centers far removed from the optimal values ($\alpha = 48°$ and $r = 3.7$ Å).

In order to examine whether the reaction mechanism for systems such as **1** occurs via efficient intramolecular general acid catalysis (IGAC) or via 'classical' general acid catalysis (GAC), we also conducted calculations for processes **6** and **7**. Where process **6** involves intermolecular proton transfer from acetic acid to the acetal, process **7** is similar to that of **6**, except that acetic acid is replaced with a molecule of water as a proton donor to the acetal (Scheme 2). Comparison of the calculated DFT activation energies in water for processes **6** and **7** with that of **1** indicates that IGAC for **1** is much more efficient than GAC for **6** and **7** ($\Delta G^{\ddagger}$ value for **1** is 24.15 kcal/mol, and for **6** and **7** are 38.55 kcal/mol and 53.14 kcal/mol, respectively). This result suggests that the proton

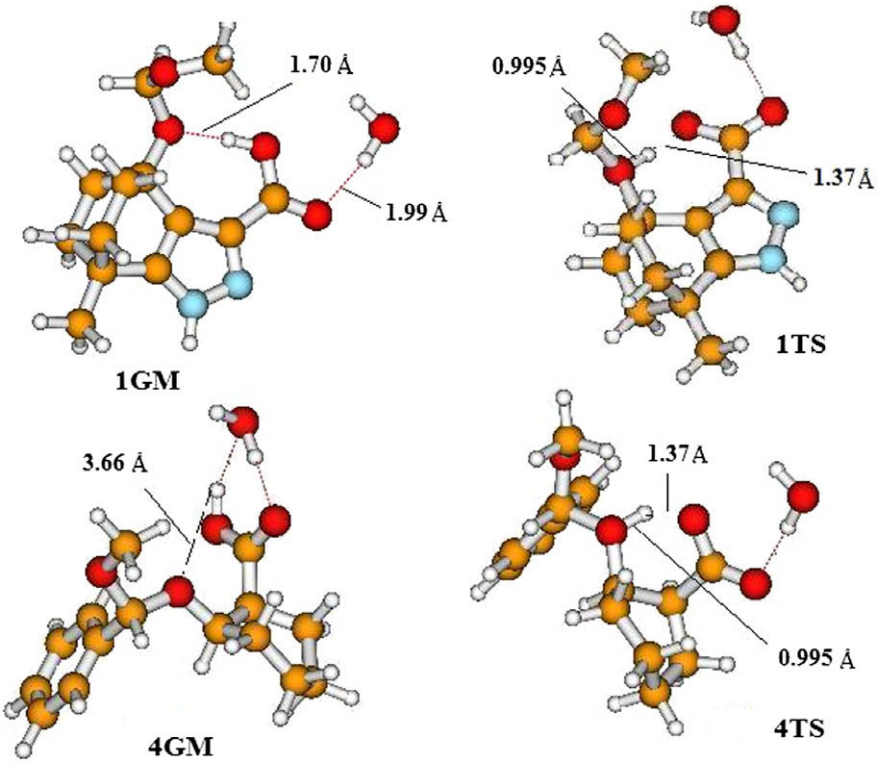

Figure 2. DFT optimized structures for the global minimum (GM) and transition state (TS) structures in intramolecular proton transfer reactions of **1** and **4**.

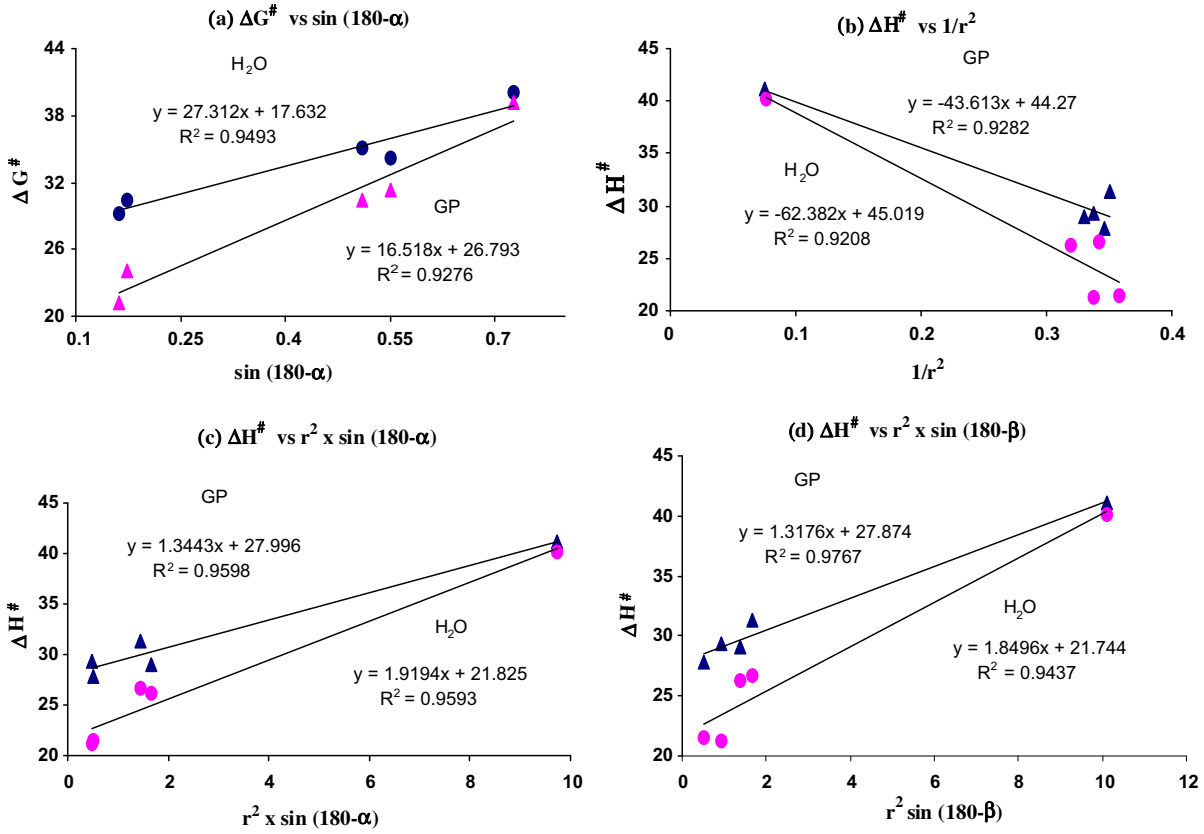

Figure 3. (a) Plot of the DFT calculated $\Delta G^{\ddagger}$ versus sin (180−α) in **1**–**5**, where α is the attack angle in the GM structure. (b) Plot of the DFT calculated $\Delta H^{\ddagger}$ versus $1/r^2$ in **1**–**5**, where r is the distance between the two reactive centers. (c) Plot of the DFT calculated $\Delta H^{\ddagger}$ versus $r^2 \times \sin(180-\alpha)$ in **1**–**5**, where α is the attack angle and r is the distance between the two reactive centers in the GM structure. (d) Plot of the DFT calculated $\Delta H^{\ddagger}$ versus $r^2 \times \sin(180-\beta)$ in **1**–**5**, where β is the attack angle in the TS and r is the distance between the two reactive centers in the GM. (GP = gas phase; H_2O = water phase).

that catalyzes cleavage of the acetal group of **1** must be supplied by the carboxyl group. Thus the mechanism in systems such as **1** is via IGAC and not via GAC. This conclusion is in perfect agreement with that drawn by Kirby.[9]

The effective molarity parameter is considered as an excellent tool to describe the efficiency of a specific intramolecular process. Since absolute EM values for processes **1**–**5** are not available[9], we sought to introduce our computational rationale for calculating these values based on the DFT calculated activation energies ($\Delta G^{\ddagger}$) of **1**–**5** and the corresponding intermolecular process **6** (Scheme 2).

Using Eq. (1)–(4), we have derived Eq. 5 which describes the EM term as a function of the difference in the activation energies of the intra- and the corresponding intermolecular processes. The values calculated using Eq. 5 for processes **1**–**5** in water are listed in Table 1.

$$EM = k_{\text{intra}}/k_{\text{inter}} \tag{1}$$

$$\Delta G^{\ddagger}_{\text{inter}} = -RT \ln k_{\text{inter}} \tag{2}$$

$$\Delta G^{\ddagger}_{\text{intra}} = -RT \ln k_{\text{intra}} \tag{3}$$

$$\Delta G^{\ddagger}_{\text{intra}} - \Delta G^{\ddagger}_{\text{inter}} = -RT \ln k_{\text{intra}}/k_{\text{inter}} \tag{4}$$

$$\text{EM} = e^{-(\Delta G^{\ddagger}_{\text{inter}} - \Delta G^{\ddagger}_{\text{intra}})/RT} \tag{5}$$

where T is 298°K and R is the gas constant.

Inspection of the EM values listed in Table 1 reveals that **5** is the most efficient process among **1**–**5** (log EM >12), and the least efficient is process **4** with log EM <1. Although the EM values of **1**–**5** were not determined experimentally, Kirby and coworkers estimated the experimental EM value for process **1** in the order of 10.[10] The DFT calculated value for **1** is 3.8×10^{10}, which is in agreement with the experimentally estimated value.[9]

In summary, we conclude that the proton transfer reactions in **1**–**5** occur via an IGAC mechanism which is driven by the following factors: (a) the distance between the two reacting centers (the carboxylic proton and the ether oxygen), (b) the attack angle α, and (c) the strength of the net hydrogen bonding between the carboxyl group and the acetal ether oxygen. In addition, the results confirm that the proton transfer rate is dependent and linearly correlated with the distance between the two reactive centers and the attack angle. This result is in accordance with Menger's 'spatiotemporal hypothesis'[4] and is in agreement with our previous studies on other proton transfer reactions.[3] Further, these results prove and support the conclusions of Kirby drawn on the dependence of the EM value on the strength of hydrogen bonding within the transition state of a proton transfer process.[9]

Further work is underway to explore the feasibility of a specific acid catalysis (SAC) mechanism for processes **1**–**5**. This will be executed by calculating the thermodynamic and kinetic properties of the entities involved in the SAC pathway and by comparing them with those in the IGAC route.

Acknowledgments

The Karaman Co. and the German-Palestinian-Israeli fund agency are thanked for support of our computational facilities. Special thanks are also given to Donia Karaman, Rowan Karaman, and Nardene Karaman for technical assistance.

Supplementary data

Supplementary data associated with this article can be found, in the online version, at doi:10.1016/j.tetlet.2010.02.062.

References and notes

1. (a) Hanson, K. R.; Havir, E. A., 3rd ed.. In *The Enzymes*; Boyer, P. D., Ed.; Academic Press: New York, 1972; Vol. 7, p 75; (b) Williams, V. R.; Hiroms, J. M. *Biochem. Biophys. Acta* **1967**, *139*, 214; (c) Klee, C. B.; Kirk, K. L.; Cohen, L. A.; McPhie, P. *J. Biol. Chem.* **1975**, *250*, 5033; (d) Hanson, K. R.; Havir, E. A. *Biochemistry* **1968**, *7*, 1904; (e) Czarin, A. W. In *Mechanistic Principles of Enzyme Activity*; Liebman, J. F., Greenberg, A., Eds.; VCH publishers: New York, 1988; (f) Nelson, D. L.; Cox, M. M. *Lehninger Principles of Biochemistry*; Worth Publishers: New York, 2003; (g) Fersht, A. *Structure and Mechanism in Protein Science. A guide to Enzyme Catalysis and Protein Folding*; W.H. Freeman and Company: New York, 1999; (h) Pascal, R. *Eur. J. Org. Chem.* **2003**, 1813; (i) Pascal, R. *Bioorg. Chem.* **2003**, *31*, 485; (j) Page, M. I.; Jencks, W. P. *Gazz. Chim. Ital.* **1987**, *117*, 455; (k) Sweigers, G. F. *Mechanical Catalysis*; John Wiley & Sons: Hoboken NJ, 2008; (l) Walsh, C. *Enzymatic Reaction Mechanisms*; San Francisco: F, 1979.
2. Kirby, A. J. *Adv. Phys. Org. Chem.* **1980**, *17*, 183. and references therein.
3. (a) Karaman, R. *Bioorg. Chem.* **2009**, *37*, 11; (b) Karaman, R. *Tetrahedron Lett.* **2008**, *49*, 5998; (c) Karaman, R. *Tetrahedron Lett.* **2009**, *50*, 452; (d) Karaman, R. *Res. Lett. Org. Chem.*, doi: 10.1155/2009/240253.; (e) Karaman, R. *Bioorg. Chem.* **2009**, *37*, 106; (f) Karaman, R. *J. Mol. Struct. (Theochem)* **2009**, *910*, 27; (g) Karaman, R. *Tetrahedron Lett.* **2009**, *50*, 6083; (h) Karaman, R. *J. Mol. Struct. (Theochem)* **2010**, *939*, 69; (i) Karaman, R. *Tetrahedron Lett.* **2009**, *50*, 7304.
4. (a) Menger, F. M. *Acc. Chem. Res.* **1985**, *18*, 128; (b) Menger, F. M.; Chow, J. F.; Kaiserman, H.; Vasquez, P. C. *J. Am. Chem. Soc.* **1983**, *105*, 4996; (c) Menger, F. M. *Tetrahedron* **1983**, *39*, 1013; (d) Menger, F. M.; Grossman, J.; Liotta, D. C. *J. Org. Chem.* **1983**, *48*, 905; (e) Menger, F. M.; Galloway, A. L.; Musaev, D. G. *Chem. Commun.* **2003**, 2370; (f) Menger, F. M. *Pure Appl. Chem.* **2005**, *77*, 1873. and references therein.
5. (a) Milstein, S.; Cohen, L. A. *J. Am. Chem. Soc.* **1970**, *92*, 4377; (b) Milstein, S.; Cohen, L. A. *Proc. Natl. Acad. Sci. U.S.A.* **1970**, *67*, 1143; (c) Milstein, S.; Cohen, L. A. *J. Am. Chem. Soc.* **1972**, *94*, 9158; (d) Borchardt, R. T.; Cohen, L. A. *J. Am. Chem. Soc.* **1972**, *94*, 9166; (e) Borchardt, R. T.; Cohen, L. A. *J. Am. Chem. Soc.* **1972**, *94*, 9175; (f) Borchardt, R. T.; Cohen, L. A. *J. Am. Chem. Soc.* **1973**, *95*, 8308; (g) Borchardt, R. T.; Cohen, L. A. *J. Am. Chem. Soc.* **1973**, *95*, 8313; (h) King, M. M.; Cohen, L. A. *J. Am. Chem. Soc.* **1983**, *105*, 2752; (i) Hillery, P. S.; Cohen, L. A. *J. Org. Chem.* **1983**, *48*, 3465.
6. (a) Bruice, T. C.; Lightstone, F. L. *Acc. Chem. Res.* **1999**, *32*, 127; (b) Lightstone, F. L.; Bruice, T. C. *J. Am. Chem. Soc.* **1997**, *119*, 9103; (c) Lightstone, F. L.; Bruice, T. C. *J. Am. Chem. Soc.* **1996**, *118*, 2595; (d) Lightstone, F. L.; Bruice, T. C. *J. Am. Chem. Soc.* **1994**, *116*, 10789; (e) Bruice, T. C.; Bradbury, W. C. *J. Am. Chem. Soc.* **1968**, *90*, 3803; (f) Bruice, T. C.; Bradbury, W. C. *J. Am. Chem. Soc.* **1965**, *87*, 4846; (g) Bruice, T. C.; Pandit, U. K. *J. Am. Chem. Soc.* **1960**, *82*, 5858; (h) Bruice, T. C.; Pandit, U. K. *Proc. Natl. Acad. Sci. U.S.A.* **1960**, *46*, 402.
7. For a recent review, see: Galli, C.; Mandolini, L. *Eur. J. Org. Chem* **2000**, 3117.
8. (a) Karaman, R. *J. Mol. Struct. (Theochem)* **2010**, *940*, 70; (b) Karaman, R. *Tetrahedron*, submitted for publication.
9. (a) Kirby, A. J. *Acc. Chem. Res.* **1997**, *30*, 290; (b) Kirby, A. J.; Parkinson, A. *J. Chem. Soc., Chem. Commun.* **1994**, 707; (c) Brown, C. J.; Kirby, A. J. *J. Chem. Soc., Perkin Trans. 2* **1997**, 1081; (d) Craze, G.-A.; Kirby, A. J. *J. Chem. Soc., Perkin Trans. 2* **1978**, 354; (e) Craze, G.-A.; Kirby, A. J.; Osborne, R. *J. Chem. Soc., Perkin Trans. 2* **1978**, 357; (f) Craze, G.-A.; Kirby, A. J. *J. Chem. Soc., Perkin Trans. 2* **1974**, 61; (g) Barber, S. E.; Dean, K. E. S.; Kirby, A. J. *Can. J. Chem.* **1999**, 792; (h) Asaad, N.; Davies, J. E.; Hodgson, D. R. W.; Kirby, A. J. *J. Phys. Org. Chem.* **2005**, *18*, 101; (i) Kirby, A. J.; Lima, M. F.; de Silva, D.; Roussev, C. D.; Nome, F. *J. Am. Chem. Soc.* **2006**, *128*, 16944; (j) Kirby, A. J.; Williams, N. H. *J. Chem. Soc., Perkin Trans. 2* **1994**, 643; (k) Kirby, A. J.; Williams, N. H. *J. Chem. Soc., Chem. Commun.* **1991**, 1643; (l) Hartwell, E.; Hodgson, D. R. W.; Kirby, A. J. *J. Am. Chem. Soc.* **2000**, *122*, 9326.
10. http://www.gaussian.com. See details of the calculation methods in Supplementary data.
11. Energy of 5 kcal/mol was needed to rotate the carboxyl group such that the attack angle increases from 48° to 88°.
12. Fife, T. H.; Przystas, T. J. *J. Am. Chem. Soc.* **1979**, *101*, 1202.